IJCRT.ORG ISSN : 2320-2882

INTERNATIONAL JOURNAL OF CREATIVE RESEARCH THOUGHTS (IJCRT)

An International Open Access, Peer-reviewed, Refereed Journal

IMPLANTATION OF DMBA COATED SILK THREAD IN ALBINO WISTAR RATS IN INDUCTION OF OVARY CANCER

1Venkata Satya Harika G, 2Dr.P.Josthna, 3Boggiti Madhuri, 4Dr. R V Suresh Kumar

1Research Scholar, 2Associate Professor , 3Research Scholar, 4Professor and University Head

1Sri Padmavathi Mahila Visva Vidyalayam (Women's University),

2Sri Padmavathi Mahila Visva Vidyalayam (Women's University),

3Sri Padmavathi Mahila Visva Vidyalayam (Women's University),

4College of Veterinary Science

Introduction

Ovary Cancer (OC) is a mainly perilous tumor amid the women's reproductive organs[1]. Our prime likelihood of OC has associated with primal aspects that can connect with biological ageing of the ovary, such as oocyte diminution, decreased ranges of anabolic steroid creation, and high degrees of passing gonadotropic hormones[2]. OC has become assumed to develop from antecedent injuries relating to the ovarian surface epithelium (OSE) or ovarian epithelial cysts that reveal structural highlights of the reproductive pathway epithelium (or Mullerian factors)[3]. The tubal epithelia, removing cells or tubal ovarian adhesions through ovulation damage or creating endometrial tissues through endometriosis, may produce Mullerian cysts[4]—besides, several events connected with ovulation linked to instigation and progression of OC. The OC includes repair of ovulation caused injuries on the surface of the ovary from the propagation of OSE, which causes the DNA injury; raising of gonadotropin levels, induced progress of OSE and ovulation-stimulated inflammation, ultimately causing the production of reactive oxygen species (ROS)[5]. Nearly 90 percentage of OCs are assumed to rise through the OSE, as the residues of ovarian neoplasms appear intently divided amid germ and stromal cell genesis. The inadequate evaluating

technique to distinguish the initial phases of the illness and its development to chemoresistance has eliminated significant changes in the endurance of bearing from OC[6].

Chemically induced animal types of ovarian tumours can exhibit oncogenesis, growth, invasion, and metastasis. 7,12-dimethylbenz[a]anthracene (DMBA) damages each follicle varieties, resulting in ovary malfunction in animals which is an element released through fuel gases and cigarette smoke[7]. It is identified that women cigarette smokers encounter ageing of the ovary in an earlier era than the non-cigarette smoking women. It is observed that the low-level DMBA revealing reason for follicle exhaustion in neonatal culture in animal's ovaries, which increasing the ovotoxicity. It is provoked at ranges that possibly associated with unaggressive DMBA exposure[8]. DMBA entails the functions of cytochromesP450 (Cyp) isoforms 1A1 and 1B1 and microsomal epoxide hydrolase (mEH) for biological modifications on the ovary toxicants. DMBA 3,4-diol, 1,2-epoxide, which happens to be the two carcinogenic and can make DNA adducts[9]. DMBA triggers the DNA mutilation in the ovaries of neonatal rat and causes its ovotoxic results[10].

Adrenomedullin (ADM) is a regulatory peptide first extracted in 1993 from human pheochromocytoma extracts by Kitamura et al.[11]. ADM is a soluble peptide and has 52 amino acids. It was purified initially from phaeochromocytoma and secreted by the adrenal medulla. Though it is a circulating hormone, it actions both paracrine or autocrine molecule with numerous biological activities like cell progress, vasodilatation, natriuresis, regulating hormone release, and antimicrobial consequences[12]. Nowadays, it is widely accepted that ADM is almost ubiquitous, with extensive cell syndication, indicating its several biological pursuits[13]. ADM is created by both stromal and tumour tissue for an autocrine/paracrine element[14]. Throughout the discrimination of macrophages, ADM is synthesized in response to pro-inflammation-related hypoxia and stimuli. Anti-inflammation results are also involved primarily in ADM, while it prevents TNF-α generation by triggering macrophages downregulating Th1-mediated autoimmune response and decreasing vascular permeability[13].

ADM is a well-defined 6-amino acid ring surrounded by a disulfide interface between 16-21 amidated and cysteines the C-terminal center, and its action is rapid [15]. ADM is indistinguishable from the quality-related peptides of amylin and calcitonin (CGRP), which are members of the amylin / CGRP / calcitonin family [16]. This similarity, along with calcitonin and other receptor peptides, allows for subsequent

cross-reactivity. An additional protein that is a major subunit of the calcitonin-like receptor (CRLR) may modify the ADM-R1 receptors ADM 2 RAMP2 and ADM-R 2 RAMP3 motor proteins [13]. The family of calcitonin quality-related peptides includes relative ADM, and the receptor regulatory protein (RAMP) complex may bind to a specific receptor marker, the calcitonin quality-related peptide receptor [17]. The two receptors ADM-R1 and ADM-R2 have been determined for AMD, which are equally formed by the significant subunits and accessory proteins. As outlined by prior reports, CGRP appeared to intervene its consequences by CGRP-α and CGRP-β[18]. It is well developed that this calcitonin receptor-like receptor (CALCRL) assets for most of the ADM and CALCA binding, and whether it binds to ADM or CALCA is determined by the sort of receptor activity modifying protein (RAMP) that is indicated notedly RAMP1, RAMP2 and RAMP3[13].

Among the exceptionally prevalent environmental factors in macrophages, ovarian cancer can be a significant hotspot for ADM lifespan, so we investigated the various possibilities of ADM in this regard. ADM is shown as several tissue developments [19]. Despite observing the limited activity of cancer cells as a stepping agent, laboratory tests confirmed that the degree of ADM increased, and beneficial results were obtained for cancer.

Materials and methods

Animal Maintenance

The in vivo study was performed according to the Institute of Animal Ethics (IAEC) and approved by the Commission (Registration No. 1677 / PO / Re / S / 2012 / CPCSEA / 3 / 6.05.16). Female Albino Wistar rats (200-240 g) were obtained from Sri Venkateswara Enterprises in Subramanya Nagar, Bangalore, India and used in this exploratory study. Female rats were placed in a polypropylene barrier covered with a metal mesh. Each mouse was kept in a room temperature (RT) environment with adequate ventilation and lighting and cared for a standard rat chow containing water.

Experimental Protocol

This review used female Wistar albino rats weighing approximately 220 ± 20 g. Female mice were mated with male rats. The next day, vaginal secretions were collected by a pipette loaded with ten µl 0.9 NaCl by inserting the tip into the rodent's vagina. A drop of vaginal fluid on the slide the ideal object was observed with a light microscope [20, 21]. Female rats supporting the estrus period were mated with male rats as the night progressed, and the next day, the male rats were isolated, and the presence of sperm in the vaginal area of the female rats was analyzed. Female rats with sperm were selected by vaginal blink on day 2 of gestation.

Preparation of DMBA-Coated Silk Suture 3-0

DMBA is heated at 124 ° C, which is the maximum value of DMBA. Place approximately 1.5-3.0 cm of silk thread on top of the melted DMBA silk suture cover with around 2-3 mg of DMBA [22].

The procedure of Ovarian Cancer Induction

Wistar rats 75-100 days old were obtained from M / S Raghavendra Enterprises in Bangalore, India. They were quarantined, modified for several weeks and stored in a controlled creature room at 25 ± 2 ° C, where the humidity in the room was maintained at 65 ± ten levels and ventilated 11 13 times/hour, 12 hours. It was enlightenment/day. Rats were cared for with ad libitium drinking and standard pellets. Treatment starts with intraperitoneal anesthesia with xylazine (8.8 mg / kg / body weight) and ketamine hydrochloride (75 mg / kg / body weight). At this stage, retroperitoneal treatment is done, and the ovaries are removed from the adipose tissue. A DMBA-covered 3.0 silk suture is implanted in the ovarian tissue, and the injury is closed again (Figure 1). After careful interaction, the mice are cared for as described under the conditions above, and the bodyweight is continuously estimated. Tumour volume and size were consistently observed after the medical procedure in the central right center of the rodent. It takes about 20 weeks from the reaction to the implant to the appearance of cancer. All movements were made by reducing the pain and experience of experienced creatures.

Infusion of Osmotic (ALZET) Pumps

Female mice measured at 220 ± 20 g were selected on the second day of growth. A micro-osmotic pump (Model 2001 Alzet siphon) was interleaved subcutaneously on the back of pregnant mice at 1.0 µl / h to give mice xylazine (8.8 mg / kg / BW) and (ketamine (75 mg / kg / BW). Smaller than regular straws include saline or saline containing 250 mcg/kg/body weight ADM22-52. This dose was selected from a study by Witlin et al. [23] And Penchalaneni et al. [24] ADM22–52 distribution of 250 mcg/kg/body weight.

Experimental Design

Female albino Wistar rats were pooled in 4 pools (n = 6). Group A saline was obtained orally by the test. Group B received ADM22-52 (250 mcg / kg / day, 14 days). The retroperitoneal region of Group C and Group D mice was treated, and the ovaries were removed from the adipose tissue. A 3.0 silk suture coated with DMBA (2-3 mg) was transplanted into the ovarian tissue, and the injury was closed again. Group C was considered disease control, and Group D was treated with 250 mcg/kg of ADM22-52 for 14 days.

The procedure of Examination with Ultrasonography

Ultrasound imaging of female mice with ovarian cancer was performed at week 20 to monitor ovarian tissue's juvenile growth and development. Mice were intravenously anesthetized with xylazine (8.8 mg / kg / body weight) and ketamine (75 mg / kg / body weight). Shave and clean the rodents from the peritoneum. The ultrasonic gel was applied to the surface of the peritoneum. Ultrasound imaging of the rat ovary was performed utilizing the Chison Q8® Versatile Ultrasound Unit (SVVU, Tirupati). Ultrasound images were taken from horizontal and vertical perspectives utilizing a multi-line transducer frequency of 7.5 to 15 MHz. Ultrasound images were stored in BMP for additional examination utilizing ImageJ® programming (National Institute of Health Sciences) [22].

Preparation and Tissue Analysis for Histopathology

Uteroimplantation sites were gathered from female rats treated with 250 µg/day of $ADM_{22–52}$ along with vehicle control. Instantly the collected uteroimplantation sites were located in 10 per cent of formaldehyde solution; later on, the uteroimplanted tissue block was dehydrated with various concentrations of isopropyl alcohol, then the tissues are embedded in paraffin and sectioned tissues into 6µm thickness lastly tissue

sections are transmitted on to the microscopic slide and stained with eosin and haematoxylin, analyzed under light microscope[25]. Related images were captured to observe for any ADM_{22-52} associated morphological changes.

Statistical Analysis

The results were denoted as mean ± SD. The effects were examined and evaluated by two analyses of variance (ANOVA) without replication for evaluating several doses of ADM antagonists. Student t-test was achieved for statistical assessment among control and treated groups. It was regard statistically significant $P<0.05$.

Results

Ovarian Cancer Induction in Rats and DMBA-Coated Silk Suture 3-0

In this review, female rats began incorporating DMBA into their ovaries to obtain a native model of epithelial ovarian cancer. DMBA 3.0 bound to silk weighs about 2-3 milligrams. After the medical procedure and DMBA transplantation into the ovaries of the mice, the mice were stored in a controlled room and taken care of to drink in standard pellets. The morphology of the right ovary was broken in each group of subjects. In addition, the bodyweight was weighed and palpation was examined on the abdomen to see nodule growth. Figure 2 shows the morphology of the right ovary of a female experimental mouse. Figure 3 shows a schematic visualization of mouse weight.

Macroscopic overview of nodules and incidence of nodule formation

Mice may be analyzed for the progression of handles formed in the central region of the mouse. In the 20th week, it can see a handle with a length of about 1.5 cm. Figure 4 shows the order of the events during this review.

Ultrasonography Imaging on Ovarian Rats

At week 20, an ultrasound scan of the mice was performed to confirm that the ovaries' size had improved. Figure 5 shows an ultrasound image of the mouse ovary. Ultrasound images showed that the average volume of the right ovary in DMBA-stimulated mice was 0.749 ± 0.141 cm 3, and the volume of the left

ovary in DMBA-free mice was 0.045 ± 0.03 cm 3 (Table). 1). these results revealed a significant variation in the size of the left and right ovaries of mice.

Histopathology examinations of Ovary Cancer induced by DMBA

At week 23, histopathology was analyzed in several mice. Primarily, histological examination was performed utilizing HE staining. Mice were analyzed, at which point the right ovary was resected and placed in 10 units of formalin. Histological examination predicts the histological assessment of the right ovary in mice. Histopathological examination was performed utilizing hematoxylin-eosin staining. Tissues are inspected utilizing a 40x amplification retardation device. The results of a proper ovarian examination at week 24 indicate a histological subtype of DMBA-induced ovarian cancer. In this subtype, cells show a polymorphic nucleus that forms near the case where the growth sequence and veins progress to growth occlusion. Appears to be displayed (Fig. 6). At week 24 of histopathological examination, DMBA induced mice to show that they had transformed ovarian cells into ovarian cancer.

DISCUSSION

This exploratory biological model was used from albino and Wistar rats. Choosing a mouse as a model for test creatures has the advantages of lower cost, more accessible care and supervision, and more obvious ethical issues than other top exploration creatures [26, 27]. In addition, specific physiological examples and the interaction of organs and hormones between humans and rats make rats excellent models for analyzing human carcinogenicity designs [27, 28]. This review was predominant in inducing the development of ovarian cancer in a group of mice given long-term DMBA hospitalization. Christ et al. in 2005 showed that immediate DMBA implantation in the rodent ovary could initiate ovarian cancer [29]. The utilize of carcinogens to induce ovarian cancer was planned utilizing DMBA-coated filamentous implants in the ovaries. Selective DMBA is a commonly used carcinogen in the screening of cancer patients and can bind directly to DNA and cause DNA mutations [26].

DMBA is an environmental carcinogen that causes ovotoxic effects on the ovaries, causing systemic loss of follicles and rapid ovarian disappointment. In general, DMBA causes ovarian folliculogenesis but is an essential progeny fragment after masking ovarian toxicity. They photographed the following parts of DMBA-induced ototoxicity in young folliculogenesis: It causes bleeding from the follicular community

and ultimately causes early ovarian failure [30]. DMBA is converted from the ovary to 3,4-diol 1,2-epoxide by members of the cytochrome P450 family of oxidases and microsome epoxide hydrolase enzymes [31]. This biologically active metabolite binds to dAdo and dGuo residues in DNA to form DMBA-DNA, causing follicle closure [32]. The latest objective evidence shows that DMBA does not cause premature ovarian failure due to high follicle initiation. Therefore, both primordial and primordial follicles in mice require rapid closure, leading to primordial follicle closure. Another important metabolite that regulates path is methionine metabolism. Methionine metabolism is an aspect of cell physiology and protects against oxidative stress and cell cycle progression [33]. Since DMBA digestion achieves expansion of ovarian ROS levels, its upregulation in DMBA-treated ovaries may be a reaction used by the ovaries to prevent oxidative stress-activated by DMBA [34]. To further support other cycles of DMBA-activated egg toxicity, qPCR has reassessed the most memorable guide genes in various cell measurements. Among the genes, Ddx5 is a member of the DEAD-box RNA erase family [35]. DMBA stimulates pore closure through higher directives of Ddx5 and Foxn3. In contrast, both Ddx5 and Foxn3 were found to induce and suppress tumorigenesis.

Ddx5 acts as an estrogen α-receptor activator to regulate its appearance and ensures cell development/persistence in cancer cell lines [35]. Although changes in quality indicators can be observed, DMBA-induced ototoxicity may be associated with various parts of follicular obstruction. Rhythmic DMBA toxicity associated with early-stage juvenile hair follicle injury, and knowledge of hair follicle fusion associated with individuals downstream of the PI3K / Akt and mTOR-labeled pathways, Akt1 phosphorylation, mTOR activation, and FOXO3 appearance It decreased further at [30]. The DNA approach is also eliminated by nucleotide extraction repair. However, if there is no improvement, it will lead to long-term changes. Point conversions, especially the conversion of adenine to thymine, and the change of base from adenine to guanine can also be grouped [36]. If these changes do not occur with silencers or oncogenes, they can lead to cell transformation and cancer growth [37]. DMBA digestion causes DNA damage that affects the growth of regulated genes, resulting in uncontrolled growth. Exocytosis occurs in all cells, including endothelial cells, and affects VEGF formation and angiogenesis [38]. As evidenced by the results of this pilot study, the DMBA transplant methods presented in this series may induce the development of ovarian cancer.

The current review analyzed the entire ADM framework from the field of rodent uterine transplantation. The utilize of ultrasound to monitor changes in ovarian volume has also shown promising results. There was a difference between the amount of right ovary obtained with DMBA and the recruitment of the left ovary that DMBA did not induce. Ovarian cancer, especially severe cancers that lead to angiogenesis, improves growth, so the development of harmful growth tissue is not well controlled. The opposite is small, especially in arterioles, because split veins have less smooth muscle than normal veins. [39]Histopathological connections examined utilizing the HE staining procedure showed that ovarian tissue found in ovarian cancer images was predicted. The results showed that ADM22-52 inhibited cell proliferation in vitro and in vivo. However, the pattern of activity of ADM22-52 in ovarian cancer has not yet been presented, and further efforts will be complemented by elucidating how ADM22-52 is reduced in ovarian cancer.

In this study, DMBA transplanted into the ovaries of female rodents may be an experimental model of epithelial ovarian cancer, and ultrasound imaging can determine the size and amount of cancer that makes up the ovaries. Light microscopy is a great way to deal with these types of pain tests. Due to this complexity, ADM is currently receiving a great deal of attention, and efforts are being made to develop the concept of principles that improve the comparison of ovarian and ovarian cancer cells.

Table legend

Table 1: Sonograms of left and right ovarian rats.

Sonogram of rat ovarian	Right ovarian	Left ovarian
Longitudinal diameter (cm)	1.707±0.149	0.523±0.095
Transversal diameter (cm)	0.954±0.078	0.392±0.053
Size (cm2)	1.614±0.212	0.215±0.038
Volume (cm3)	0.749±0.141	0.045±0.03

Data are presented in the form of average and standard deviation (Mean± SD).

Figure Captions

Figure 1: Procedure of ovarian cancer induction

Figure 2: Morphology of Right Ovaries of Ovary Tumor-induced Experimental Animals

Figure 3: Effect of ADM22–52 on Bodyweight (g) of Ovary Tumor-induced Experimental Animals.

Figure 4: Incidence of nodule formation.

Figure 5: Sonograms of ovarian rats.

Figure 6: Histological report of the right ovary.

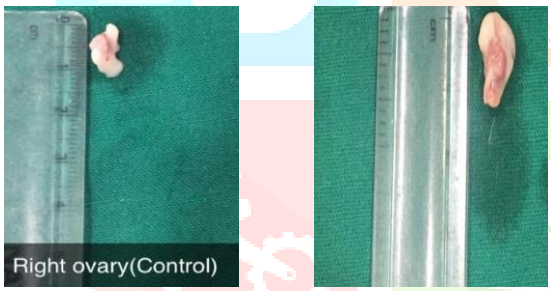

FIGURE 1

Group A **Group B**

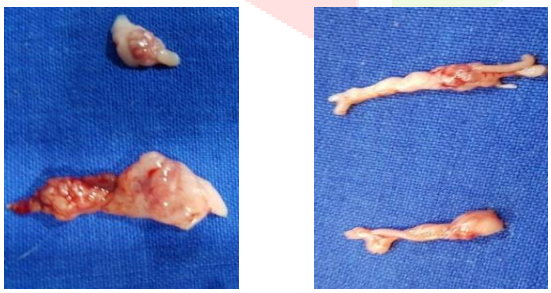

FIGURE 2

Group C **Group D**

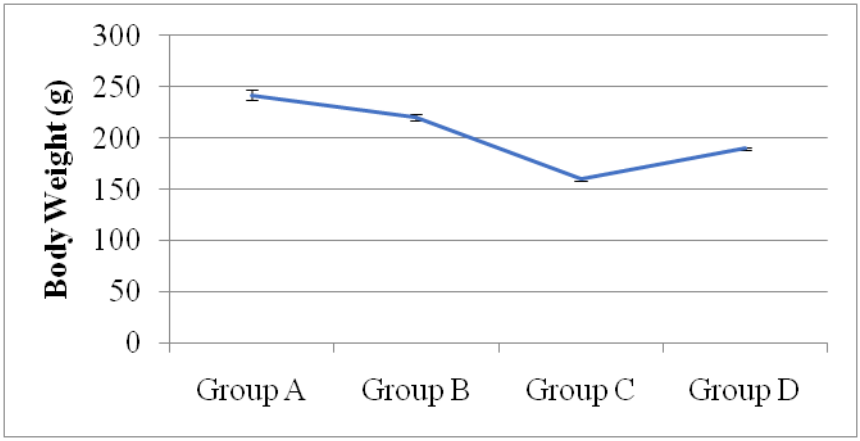

FIGURE 3

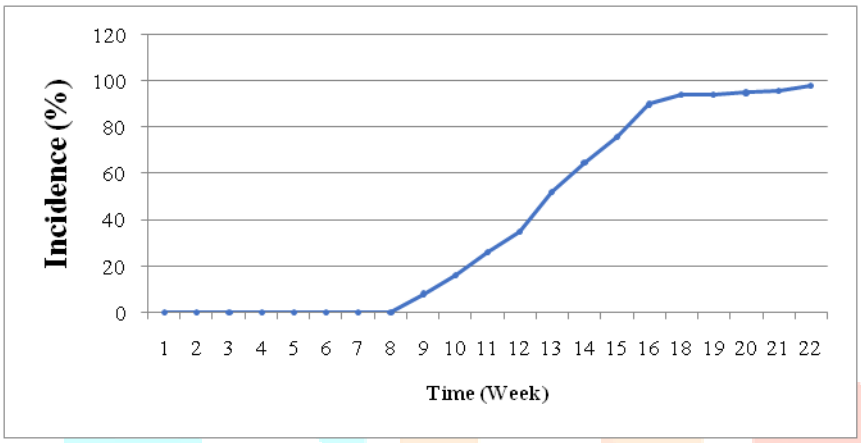

FIGURE 4

FIGURE 5

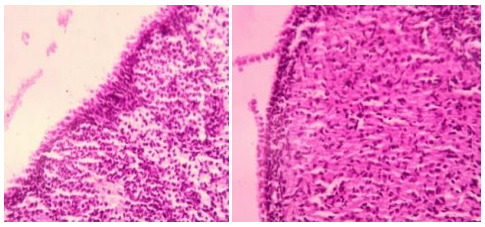

GROUP A

GROUP B

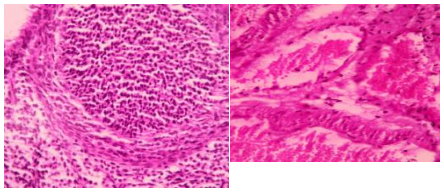

GROUP C

GROUP D

FIGURE 6